Available online at www.sciencedirect.com
SCIENCE DIRECT®
Journal of the European Ceramic Society 25 (2005) 3353–3359
www.elsevier.com/locate/jeurceramsoc

Microstructure and mechanical properties of silicon nitride ceramics prepared by pressureless sintering with $MgO–Al_2O_3–SiO_2$ as sintering additive

Xue-Jian Liu*, Zhi-Yong Huang, Qi-Ming Ge, Xing-Wei Sun, Li-Ping Huang

Shanghai Institute of Ceramics, Chinese Academy of Sciences, Shanghai 200050, China

Received 23 April 2004; received in revised form 4 August 2004; accepted 15 August 2004

Abstract

The microstructure and mechanical properties of pressureless sintered Si_3N_4 ceramics prepared both by conventional ball-milling and planetary high-energy ball-milling for a sintering additive from the $MgO–Al_2O_3–SiO_2$ system were investigated by XRD, SEM, TEM, HRTEM, and EDS. For pressureless sintered Si_3N_4 ceramics prepared by planetary ball-milling, a flexure strength of 1.06 GPa, Vickers hardness of 14.2 GPa, and fracture toughness of 6.4 $MPa·m^{0.5}$ were achieved. The microstructure of the sintered materials consists of elongated grains with almost identical size and aspect ratio that uniformly distributed throughout the body. The improved mixing efficiency by planetary ball-milling has simply reduced the particle size and improved the distribution of sintering additives, leading to a slightly improved densification and microstructural homogenization that are responsible for the promising properties of Si_3N_4 ceramics. In comparison with traditional ball-milling route, the planetary high-energy ball-milling is an efficient processing to produce high homogeneous microstructure and promising mechanical properties.

Keywords: Pressureless sintering; Microstructure; Mechanical properties; Si_3N_4

1. Introduction

Silicon nitride based ceramics (Si_3N_4) have been widely studied because of their potential applications as structural components at both room and elevated temperatures.[1–8] Pressureless sintering is now commonly used to fabricate dense Si_3N_4 parts with complex shapes because of its economic advantages over hot pressing and the improvement in thermal mechanical properties as compared to those achieved by reaction-bonded sintering.[6–8] However, the covalent nature of Si–N bonding requires the use of sintering additives, such as metal oxides and rare-earth-metal oxides, to promote densification through liquid-phase sintering. During sintering, the oxide additives react with silica (SiO_2) on the surface of Si_3N_4 particles to form a vitreous flux at the sintering temperature assisting mass transport during densification. Thus, the sintering behavior of Si_3N_4, which includes densification, α-to-β phase transformation, and grain growth, is influenced substantially by the amount and chemistry of the liquid phase.[2]

As well known, the room-temperature properties of Si_3N_4 ceramics are mainly determined by the two microstructural characteristics, aspect ratio and grain size of the β-phase, and that the high-temperature strength is controlled particularly by the characteristics of the grain boundary phase.[9] Consequently, rare earth oxides were commonly used as the additives of Si_3N_4 for the improvement of high temperature mechanical properties. Since adding a rare earth alone (<10 wt.%) is not as effective as a sintering aid concurrent additions of rare earth and metal oxides are usually done to increase the sinterability.[10] These additives, however, form glassy grain-boundary phases in the dense body which deteriorate high temperature mechanical properties of ceramics

* Corresponding author. Tel.: +86 2152 414220; fax: +86 2152 413903.
E-mail address: xjliu@mail.sic.ac.cn (X.-J. Liu).

0955-2219/$ – see front matter © 2004 Elsevier Ltd. All rights reserved.
doi:10.1016/j.jeurceramsoc.2004.08.025

such as creep and high temperature strength.[2–4] Several methods to improve the mechanical properties at elevated temperature have been proposed: use fewer additives, crystallize the glassy phase by heat treatment, and use an adequate composition through which the additives dissolve in Si_3N_4 grains after sintering. With these methods, the high temperature properties can be improved by minimizing the volume of the glassy phase.[4] Y_2O_3 and Al_2O_3 are the most commonly used successful additives.[2–6] Since Y_2O_3 is expensive, many alternative additives have been investigated to replace it and to obtain crystalline grain-boundary phases.[7] In fact, liquid-phase sintering process of Si_3N_4 has been widely investigated on the addition of MgO, Y_2O_3, Al_2O_3–Y_2O_3 and other oxides.[1–8] However, there are few studies on the liquid-phase sintering of Si_3N_4 for a sintering additive from the MgO–Al_2O_3–SiO_2 system.

For strong covalent bonded structural ceramics, e.g., Si_3N_4 and SiC, the introduction of sintering additives is a crucial step in the production process, because they must be homogeneously distributed throughout the ceramic matrix.[11–12] In fact, inhomogeneities generally formed at the earlier stage and became even larger during the subsequent processing, which causes strength degradation and lower reliability.[5] A crucial step is to find a powder blending route able to produce high homogeneity in powder mixtures. Conventionally, the starting powders are mixed by general ball-milling to reduce particle size and drive homogeneous distribution of sintering aids in a polyethylene bottle or nylon jar.[2–7] However, the traditional ball-milling techniques usually take a long time and produce green compacts with poor homogeneity.[12] Both chemical methods and wet mixing routes have been investigated with the aim to improve the homogeneity of the additives' distribution.[12–16] Advantages of the chemical methods, e.g., coprecipitation, coating of the additives in situ on Si_3N_4 particles, are a better homogeneity of sintering aids and the consequent possibility to reduce the amount of additives.[12–14] However, in some cases the chemical processes are expensive, and there are some technological difficulties concerning their scale-up to industrial mass production. On the other hand, various wet mixing routes, e.g., mechanical, ultrasonic, and attrition mixing, have been used to introduce sintering aids in Si_3N_4 suspensions and their impact on the surface composition and surface coverage were investigated.[16] The results showed that the attrition mixing and ultrasonication resulted in the more efficient processing routes to distribute the sintering aids on the starting Si_3N_4 powders, but the effects of milling processing on the microstructure and mechanical properties were not reported. Oliveira et al.[17] showed that planetary milling was more efficient in deagglomerating of Si_3N_4-based suspensions compared with ball milling, enabling a significant decrease of the milling period required to obtain full dispersion. Recently, planetary milling process has been widely used as a non-equilibrium mechanical processing technique to synthesis nanostructured ceramic powders.[18–22] However, extensive study concerning the microstructure and mechanical properties of structural ceramics produced through planetary milling has been few reported in the literature.

In the present study, the sintering behavior and the influence of ball-milling methods on the microstructure and mechanical properties of Si_3N_4 ceramics prepared by pressureless sintering were investigated for a sintering additive from the MgO–Al_2O_3–SiO_2 system. The aim of this work is to compare the microstructure and mechanical properties of Si_3N_4 ceramics prepared by different blending methods and to verify that the planetary high-energy ball-milling is an efficient processing to distribute the sintering additives on the starting powders, leading to homogeneous microstructure and promising mechanical properties.

2. Experimental procedure

Commercially available Si_3N_4 powder (E-10, UBE Industries, Japan, 1.43 wt.% oxygen content, 93% wt.% α phase) was mixed with 3 wt.% MgO (99.9%), 1.5 wt.% Al_2O_3 (99.9%) and 3.5 wt.% SiO_2 (99.9%) additives, blended by general ball-milling and planetary high-energy ball-milling respectively in a Si_3N_4 container using Si_3N_4 balls and ethanol as media. The ratio of powder to milling-ball is 1:3 in weight. The content of ethanol is 80% of the dry ceramic powder. The ball-milling conditions for conventional milling are 60 rpm for 1 week while that for planetary milling are 250 rpm for 5 h. Then, the mixtures were dried and sieved passed through a 200-mesh screen. Powders were compressed in a steel die under 10 MPa to form 5 mm × 5 mm × 40 mm green compacts. The compacts were pressed isostatically under 200 MPa for 1 min and then sintered in a graphite resistance furnace under atmosphere pressure of nitrogen at 1780 °C for 1.5–3 h.

The particle size distribution and specific surface area of ceramic powders before and after milling were determined by light-permeating-sedimentation particle size analyzer (Model SICAS-4800) and BET nitrogen adsorption method (Model ASAP-2010), respectively. The bulk density of sintered specimens was measured by the Archimedes methods. The relative density was calculated based on the theoretical density of each individual constituent and its content. The density of 2.0 g/cm^3 was used for silica. The phase identification was performed from spectrum collected by an X-ray diffractometer (XRD, D/max 2550 V) using Cu Kα radiation. The microstructure photographs of ceramic powders and sintered bodies were observed by field emission scanning electron microscopy (SEM, Model JSM-6700F). For microstructure observations, the samples were cut and polished and then etched in molten NaOH for ∼1 min, examined by SEM, and analyzed with LEICA QWin image analysis software (LEICA Microsystems) using the SEM micrographs. About 1500 grains from each sample were measured. The grain boundary phases were examined with high resolution transmission electron microscopy (HRTEM, Model JEM-2010) equipped with an energy dispersive X-ray

spectroscopy (EDS). HRTEM specimen was prepared by cutting and grinding them to a thickness of ~100 μm, followed by dimpling and ion beam milling. Test samples for mechanical properties were machined into bars with dimension of 3 mm × 4 mm × 35 mm before a three-point bending test was conducted at a loading rate of 0.5 mm/min on a universal testing machine (Instron-1195). Using a polished surface, Vickers microhardness and fracture toughness were determined by the indentation method (Model AVK-A). An initial precrack of 1 mm in depth was cut using a diamond blade (0.15 mm in thickness). No less than 12 bars were tested for each measurement.

3. Results and discussion

Fig. 1 shows the particle size distributions of Si_3N_4 powders before and after milling. One can see that the particle size of the powder mixtures after planetary high-energy ball-milling decreases markedly. Correspondingly, the effect of general milling on the particle characteristics is weak. BET surface areas for as-available powders and after general and planetary ball-milling are 9.5, 10.1, and 18.1 m^2/g, respectively, an indicative of BET surface area increases in a factor of two after planetary ball-milling. These results indicate that planetary ball-milling has a prominent impact for milling the powders. Fig. 2 gives the SEM morphological photographs of Si_3N_4 powders before and after milling, which are in good agreement with the results shown in Fig. 1.

Fig. 3 shows the relative density and linear shrinkage of the Si_3N_4 specimens prepared by planetary high-energy ball-milling and sintered at 1500–1780 °C for 1.5 h. As can be seen, the linear shrinkage of the sample sintered at 1500 °C for 1.5 h was very small. Due to the formation of ample liquid phase which assists mass transport and rearrangement, the densification of the Si_3N_4 specimens proceeded quickly with the increase of sintering temperature. The relative densities of the samples sintered at 1750 and 1780 °C for 1.5 h were 98.4 and 99.1%, respectively. The density above 99.7% of theoretical was attained at sintering temperature of 1780 °C for 3 h. After sintering at 1780 °C for 1.5 h, the specimen consisted of β-Si_3N_4 and no other phase was detected by XRD analysis, as shown in Fig. 4. The growth kinetics of β-Si_3N_4 grains in Si_3N_4 ceramics containing a liquid phase have been studied by many researchers.[23–29] The α–β transformation is believed to occur after solution of fine α grains and subsequent reprecipitation as β-phase in a liquid phase formed from the sintering additive.

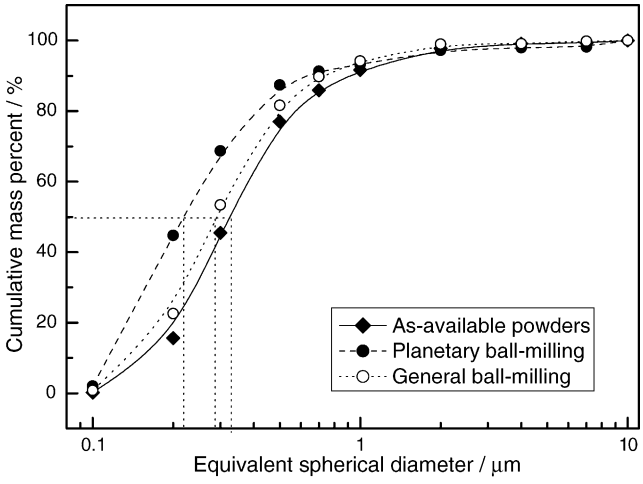

Fig. 1. The particle size distribution of ceramic powders before and after milling.

Table 1 shows the relative density and mechanical properties of Si_3N_4 ceramics prepared by planetary high-energy ball-milling and sintered at 1780 °C for various soaking time. For comparison, the results of Si_3N_4 ceramics prepared by general ball-milling were also displayed. As can be seen, with increasing the sintering temperature and soaking time, the relative density and mechanical properties of Si_3N_4 ceramics were expectantly improved. For Si_3N_4 ceramics sintered at 1780 °C for 3 h, a density near full densification (99.7% of the theoretical), flexure strength of 1.06 GPa, Vickers hardness of 14.2 GPa, and fracture toughness of 6.4 MPa $m^{0.5}$ were achieved. It is noteworthy that Si_3N_4 ceramics with flexure strength above 1 GPa is prepared by pressureless sintering with planetary ball-milling process that is comparable to that of achieved by previous hot-press or gas-pressure sintering.[4–5] By comparison, the relative density and mechanical properties of Si_3N_4 ceramics prepared by general ball-milling were evidently degraded. Moreover, the standard deviations of mechanical properties for planetary ball-milling were somewhat smaller than that for general ball-milling.

It was reported that elongated β-grains are commonly developed in the sintered Si_3N_4 ceramics because the growth of β-grain is anisotropic with the *c*-axis growth rates generally exceeding those normal to the prism faces.[23] Fig. 5 presents the SEM micrographs of fractured surfaces and polished and etched surfaces of Si_3N_4 ceramics prepared by planetary ball-milling, respectively; while that for general ball-milling Si_3N_4 were shown in Fig. 6. As expected, both the specimens were consisted primarily of randomly oriented elongated β-Si_3N_4 grains. The main differences were the grain size distribution and microstructural homogeneity. An image analysis using the micrographs showed that the

Table 1
Relative density and mechanical properties of Si_3N_4 ceramics prepared at various conditions

Samples no.	Relative density (%)	Flexure strength (MPa)	Vickers hardness (GPa)	Fracture toughness (MPa·$m^{0.5}$)
1750 – 1.5h – P*	98.4	818 ± 72	13.1 ± 1.4	5.8 ± 0.6
1780 – 1.5h – P*	99.1	925 ± 48	13.5 ± 1.2	6.2 ± 0.5
1780 – 3h – P*	99.7	1059 ± 37	14.2 ± 1.0	6.4 ± 0.5
1780 – 3h – G**	99.2	918 ± 53	13.6 ± 1.3	6.3 ± 0.5

* P: planetary high-energy ball-milling.
** G: general ball-milling.

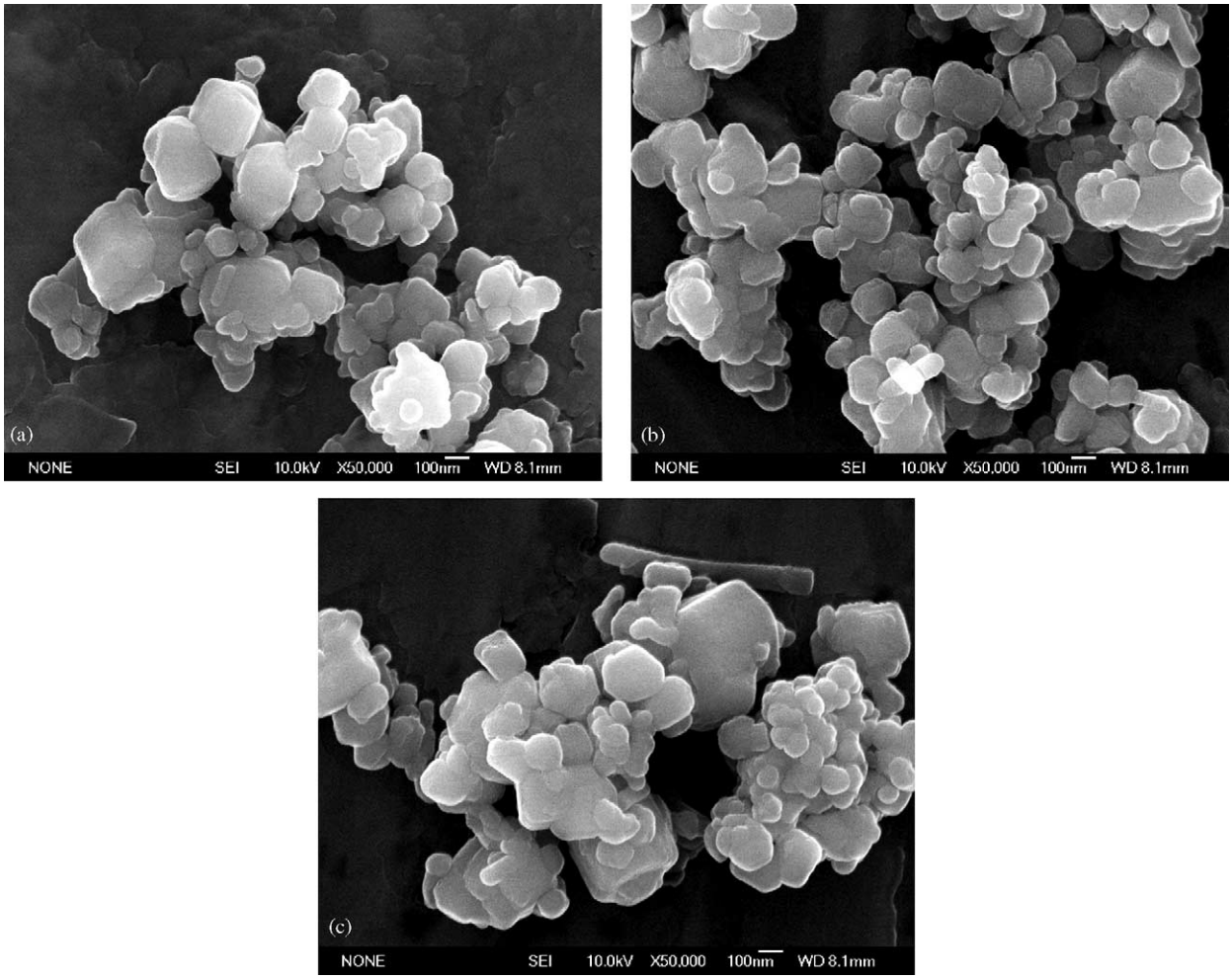

Fig. 2. SEM photographs of ceramic powders before and after milling: (a) before milling, (b) after planetary ball-milling, (c) after general ball-milling.

average diameter of the elongated grains for planetary ball-milling Si_3N_4 was 0.7 μm with an aspect ratio of 6.2. For general ball-milling Si_3N_4, a microstructure similar to that for planetary ball-milling Si_3N_4 was observed, as shown in Fig. 6. The average diameter and aspect ratio of the elongated

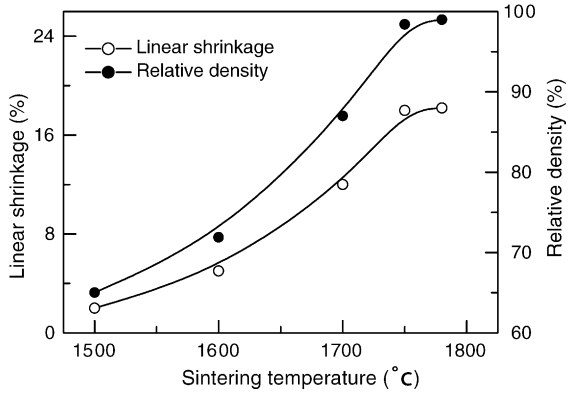

Fig. 3. Densification kinetics of Si_3N_4 compacts sintered at 1500–1780 °C for 1.5 h.

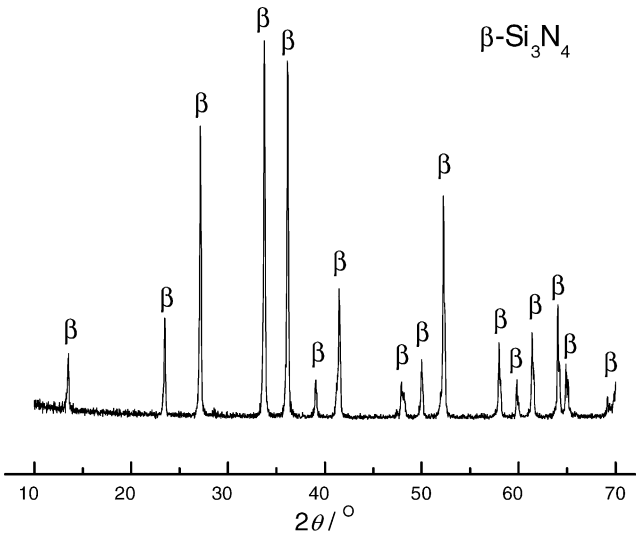

Fig. 4. XRD patterns of Si_3N_4 ceramics sintered at 1780 °C for 1.5 h.

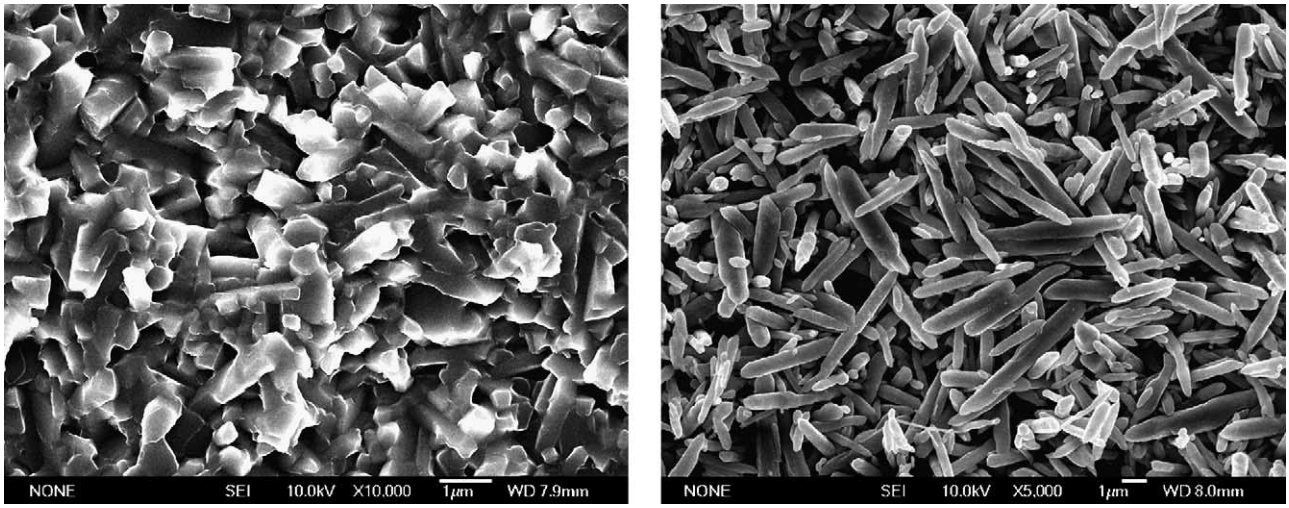

Fig. 5. SEM micrographs of fractured surface and polished and etched surfaces of Si_3N_4 ceramics prepared by planetary ball-milling.

Si_3N_4 grains almost remained about the same; however, the distribution of the grain diameter became wider a little and some exaggeratedly grown grains were found in the local areas. Considering the same conditions expect their ball-milling processing, the development of larger elongated grains is therefore believed to be due to the local enrichment of sintering additives that form eutectic liquid phase at high temperature. The abundance of liquid phase accelerates the mass transport and thus abnormal grain growth occurs in the partial areas. For planetary high-energy ball-milling, the sintering additives were adequately mixed together with Si_3N_4 powders, which inhibited the abnormal growth of β-Si_3N_4 grains. As a result, the microstructure of the sintered body consists of elongated grains with almost identical grain size and aspect ratio that uniformly distributed throughout the body, as shown in Fig. 5.

It is known that liquid phase sintered Si_3N_4 has a continuous oxynitride glassy phase surrounding the Si_3N_4 grains. Because the thermal expansion coefficient for bulk oxynitride glass is higher than that of Si_3N_4, it is very possible that the grain boundary glassy phase is under a residual tensile stress. Since a larger grain is associated with a higher residual stress in the surrounding glass, it is spontaneously believed that stress-induced microcracking predominantly occurs in exaggerated-grains-containing materials than in uniform grains material.[30–31] Therefore, the differences in the mechanical properties of Si_3N_4 ceramics produced by different processing seem to arise partially from the changes in the homogenization of the grain size and their distribution throughout the bodies. Besides, the improvement of the sinterability of Si_3N_4 with the improved homogeneity of the sintering additives distributed over the matrix and the resultant higher relative density are quite easily suggested partially responsible for the improvement of the mechanical properties. The densification of Si_3N_4 is controlled mainly by particle rearrangement and solution-reprecipitation, both of which are

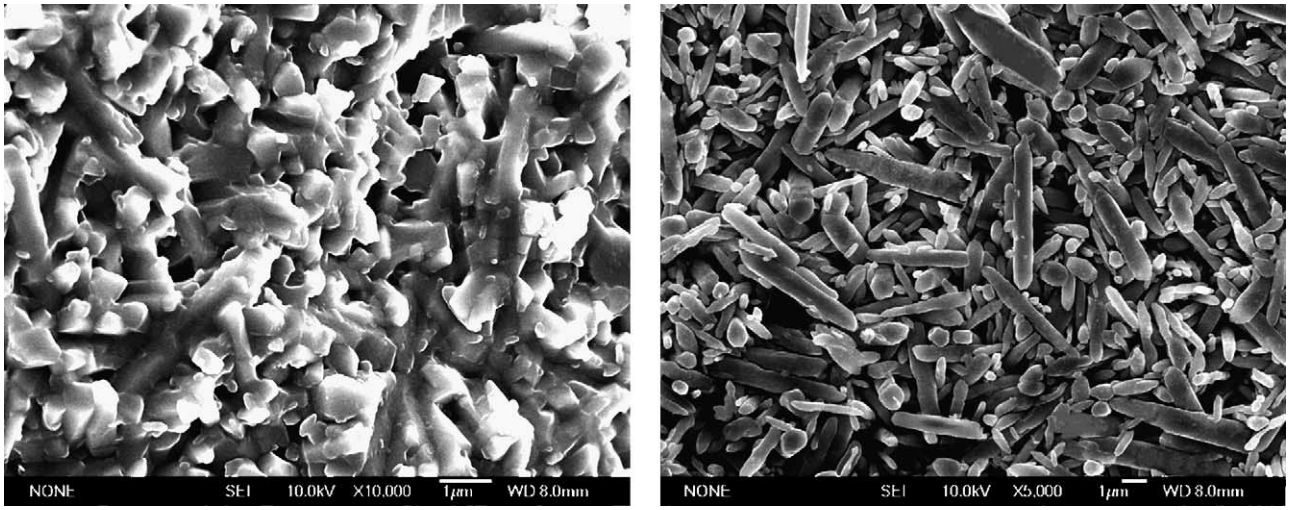

Fig. 6. SEM micrographs of fractured surface and polished and etched surfaces of Si_3N_4 ceramics prepared by general ball-milling.

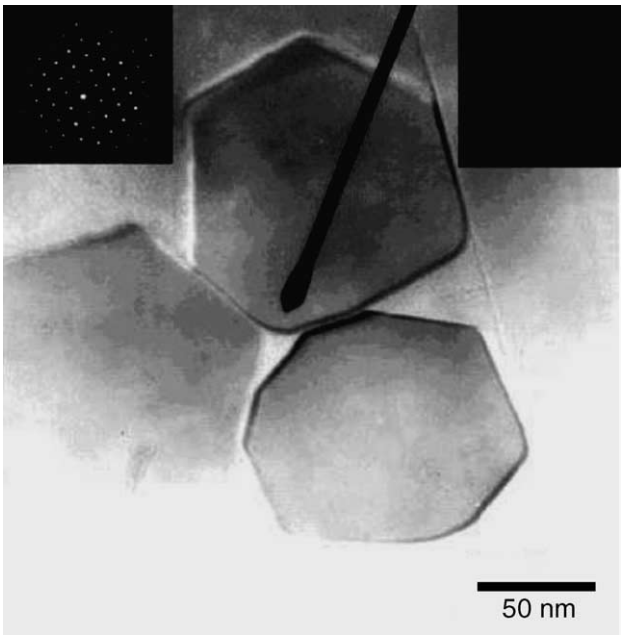

Fig. 7. TEM image and electron diffraction pattern (inset) of the grain (left upper) and triple-grain regions (right upper) of Si_3N_4 ceramics prepared by planetary ball-milling.

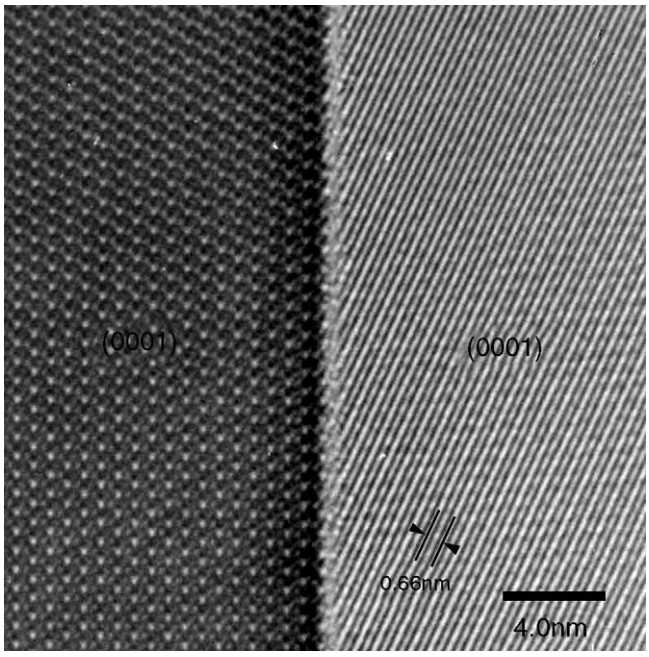

Fig. 9. HRTEM micrograph of Si_3N_4 ceramics prepared by planetary ball-milling showing residual amorphous glass along two-grain boundary.

enhanced by liquid-phase formation at the grain boundary. The densification of Si_3N_4 during sintering is known to be inhibited by the impingement effect of rodlike β-Si_3N_4 grain growth.[32] Similarly, the exaggerated grains prevent the densification of general ball-milling Si_3N_4. For planetary ball-milling Si_3N_4, the uniformly distributed sintering additives contribute to particle rearrangement, and thus improve densification. Moreover, the smaller scatter in mechanical properties for planetary ball-milling are also resulted from the improved microstructure homogeneity and reliability. So, it may be concluded that the improved milling has simply reduced the particle size and improved the distribution of sintering additives, leading to a slightly improved densification and microstructural homogenization.

Additionally, TEM was used to examine Si_3N_4–Si_3N_4 and Si_3N_4–glass interfaces, as indicated in Fig. 7. This examination showed that the presence of a large three-grain junction with an amorphous phase that is typical of Si_3N_4-based materials. Fig. 8 gives the compositions of the grains and the grain boundary identified by EDS. As expected, the elongated grain contains only Si and N; the triple-grain junction contains Si, Mg, and Al, with a large amount of oxygen and a small amount of nitrogen. In contrast, nearly all of the Mg, Al and O elements remained in the triple points. These results suggest that the liquid phase, through which needle-like grains were developed by a solution and precipitation mechanism, formed an amorphous Mg–Al–Si–O–N grain-boundary phase. Fig. 9 is an HRTEM image of Si_3N_4 ceramics prepared by planetary ball-milling, which shows the absence of residual amorphous glass at the Si_3N_4–Si_3N_4 two-grain boundary.

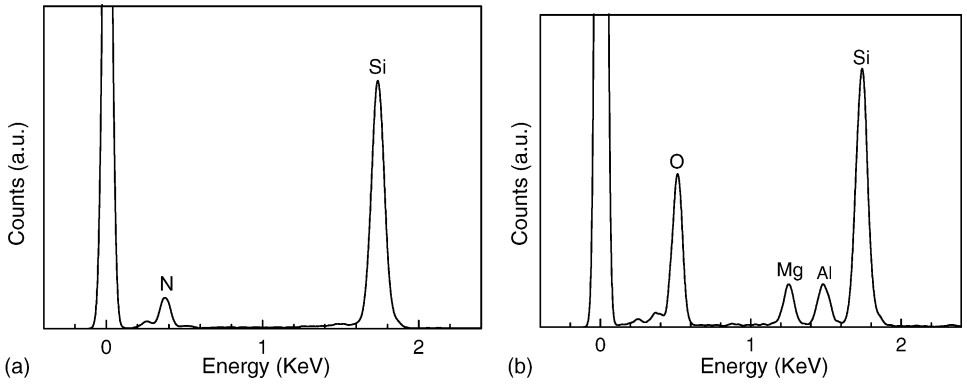

Fig. 8. Energy-dispersive X-ray spectra (EDS) of Si_3N_4 ceramics prepared by planetary ball-milling showing relative amounts of various elements in (a) grain, (b) grain boundary.

4. Conclusions

In comparison with traditional ball-milling route, the planetary high-energy ball-milling is an efficient process to blend ceramic powders and, thus, to produce homogeneous microstructure and to improve the mechanical properties of sintered ceramics. By planetary ball-milling, a flexure strength of 1.06 GPa, Vickers hardness of 14.2 GPa, and fracture toughness of 6.4 MPa $m^{0.5}$ were attained by pressureless sintered Si_3N_4 ceramics with $MgO–Al_2O_3–SiO_2$ additives. The SEM micrograph reveals that the microstructure of the sintered body consists of elongated grains with almost identical grain size and aspect ratio that uniformly distributed throughout the body. TEM examination reveals that the presence of a large three-grain junction with an amorphous phase and the absence of residual amorphous glass at the two-grain junction. The improved densification and microstructural homogenization resulted from the improved distribution of sintering additives are responsible for the promising mechanical properties of the specimen.

Acknowledgements

Supported by the High-Tech Development Program of China (No. 863-3-333030) and the Scientific Development Fund of Shanghai Municipality (No. 0152nm031, 04DZ14002), China.

References

1. Biswas, S. K. and Riley, F. L., Gas pressure sintering of silicon nitride powder coated with Al_2O_3 and TiO_2. *J. Am. Ceram. Soc.*, 2003, **86**(2), 212–216.
2. Yang, J. F., Ohji, T. and Niihara, K., Influence of yttria alumina content on sintering behavior and microstructure of silicon nitride ceramics. *J. Am. Ceram. Soc.*, 2000, **83**(8), 2094–2096.
3. Park, H., Kim, H. E. and Niihara, K., Microstructural evolution and mechanical properties of Si_3N_4 with Yb_2O_3 as a sintering additive. *J. Am. Ceram. Soc.*, 1997, **80**(3), 750–756.
4. Hirosaki, N., Okada, A. and Matoba, K., Sintering of Si_3N_4 with the addition of rare-earth oxides. *J. Am. Ceram. Soc.*, 1988, **71**(3), 144–147.
5. Lencces, Z., Guicciardi, S., Melandri, C. and Bellosi, A., Preparation, microstructure, and mechanical property relationships in silicon nitride based ceramics. *Br. Ceram. Trans.*, 1995, **94**(4), 138–145.
6. Almeida, J. C., Fonseca, A. T., Correia, R. N. and Baptista, J. L., Pressureless sintering of silicon nitride with additives of the $Y_2O_3–Al_2O_3–SiO_2$ system. *Mater. Sci. Eng.*, 1989, **A109**, 395–400.
7. Tunaboylu, B. and Varner, J. R., Pressureless sintering and characterization of Si_3N_4 containing La_2O_3–SrO as an additive. *J. Mater. Sci. Lett.*, 1995, **14**, 1246–1249.
8. Lee, C. J. and Kim, D. J., Effect of α-Si_3N_4 particle size on the microstructural evolution of Si_3N_4 ceramics. *J. Am. Ceram. Soc.*, 1999, **82**(3), 753–756.
9. Wotting, G. and Ziegler, G., Influence of powder properties and processing conditions on microstructure and mechanical properties of sintered Si_3N_4. *Ceram. Int.*, 1984, **10**(1), 18–22.
10. Tani, E., Umebayashi, S., Kishi, K., Kobayashi, K. and Nishijima, M., Gas-pressure sintering of Si_3N_4 with concurrent addition of Al_2O_3 and 5 wt.% rare earth oxide: high fracture toughness Si_3N_4 with fiber-like structure. *Am. Ceram. Soc. Bull.*, 1986, **65**(9), 1311–1315.
11. Bellosi, A., Galassi, C. and Fabbriche, D. D., Sintering characteristics of Si_3N_4 powders. *High Temp. High Pressures*, 1988, **20**, 335–343.
12. Bellosi, A., Monteverde, F. and Babini, G. N., Influence of powder treatment methods on sintering, microstructure and properties of Si3N4-based materials. In *Engineeting Ceramics '96: Higher Reliability Through Processing, Vol 25*. Kluwer Academic Publishers, 1996, pp. 197–212.
13. Bertoni, F., Galassi, C., Ardizzone, S. and Bianchi, C. L., Surface modification of Si3N4 powders by coprecipitation of sintering aids. *J. Am. Ceram. Soc.*, 1999, **82**(10), 2653–2659.
14. Lang, F. F., Powder processing science and technology for increased reliability. *J. Am. Ceram. Soc.*, 1989, **72**(1), 3–15.
15. Jeong, Y. K., Nakahira, A., Morgan, P. E. D. and Niihara, K., Effect of milling conditions on the strength of alumina-silicon carbide nanocomposites. *J. Am. Ceram. Soc.*, 1997, **80**(5), 1307–1309.
16. Bertoni, F., Galassi, C., Ardizzone, S. and Bianchi, C. L., Water-based Si_3N_4 suspensions. Part II. Effect of wet mixing/milling processes on the addition of the sintering aids. *J. Mater. Res.*, 2000, **15**(1), 164–169.
17. Oliveira, M. L. L., Chen, K. and Ferreira, J. M. F., Influence of the deagglomeration procedure on aqueous dispersion, slip casting and sintering of Si_3N_4-based ceramics. *J. Eur. Ceram. Soc.*, 2002, **22**(9/10), 1601–1607.
18. Zhang, Q. and Saito, F., Mechanochemical synthesis of lanthanum aluminate by grinding lanthanum oxide with transition alumina. *J. Am. Ceram. Soc.*, 2000, **83**(2), 439–441.
19. Lee, J., Zhang, Q. and Saito, F., Mechanochemical synthesis of lanthanum oxyfluoride from lanthanum oxide and lanthanum fluoride. *J. Am. Ceram. Soc.*, 2001, **84**(4), 863–865.
20. Fukuda, K., Inoue, S. and Yoshida, H., Substitution of sodium and silicon in tricalcium aluminate. *J. Am. Ceram. Soc.*, 2003, **86**(1), 112–114.
21. Pan, X., Chen, Y., Ma, X. and Zhu, L., Phase transformation of nanocrystalline anatase powders induced by mechanical activation. *J. Am. Ceram. Soc.*, 2004, **87**(6), 1164–1166.
22. Hampsey, J. E., De Castro, C. L., McCaughey, B., Wang, D., Mitchell, B. S. and Lu, Y., Preparation of micrometer- to sub-micrometer-sized nanostructured silica particles using high-energy ball milling. *J. Am. Ceram. Soc.*, 2004, **87**(7).
23. Hwang, C. J. and Tien, T.-Y., Microstructure development in silicon nitride ceramics. *Mater. Sci. Forum*, 1989, **47**, 84–109.
24. Lee, D. D., Kang, S. J. L. and Yoon, D. N., Mechanism of grain growth and α–β′ transformation during liquid phase sintering of β′-sialon. *J. Am. Ceram. Soc.*, 1988, **71**(9), 803–806.
25. Mitomo, M. and Uenosono, S., Microstructure development during gas pressure sintering of α-silicon nitride. *J. Am. Ceram. Soc.*, 1992, **75**(1), 103–108.
26. Lai, K-R. and Tien, T-Y., Kinetics of β-Si_3N_4 grain growth in Si_3N_4 ceramics sintered under high nitrogen pressure. *J. Am. Ceram. Soc.*, 1993, **76**(1), 91–96.
27. Einarsrud, M. A. and Mitomo, M., Mechanism of grain growth of β-SIAlON. *J. Am. Ceram. Soc.*, 1993, **76**(6), 1624–1626.
28. Kramer, M., Topotacally oriented α-Si_3N_4 cores in sintered β-Si_3N_4. *J. Am. Ceram. Soc.*, 1993, **76**(6), 1627–1629.
29. Kramer, M., Hoffmann, M. J. and Petzow, G., Grain-growth of silicon nitride dispersed in a oxynitride glass. *J. Am. Ceram. Soc.*, 1993, **76**(11), 2778–2784.
30. Li, C. W., Lui, S. C. and Goldacher, J., Relation between strength, microstructure, and grain-bridging characteristics in situ reinforced silicon nitride. *J. Am. Ceram. Soc.*, 1995, **78**(2), 449–459.
31. Iizuka, T., Murao, T., Yamamoto, H. and Kita, H., Microstructure and properties of Mo_5Si_3-particle-reinforced Si_3N_4-matrix composites. *J. Am. Ceram. Soc.*, 2002, **85**(4), 954–960.
32. Abe, O., Sintering process of Y_2O_3 and Al_2O_3-doped Si_3N_4. *J. Mater. Sci.*, 1990, **25**, 4018–4026.